Journal of Bacteriology

The SigF Regulon in *Mycobacterium smegmatis* Reveals Roles in Adaptation to Stationary Phase, Heat, and Oxidative Stress

Anja Hümpel, Susanne Gebhard, Gregory M. Cook and
Michael Berney

Updated information and services can be found at:
http://jb.asm.org/content/192/10/2491

These include:

CONTENT ALERTS   Receive: RSS Feeds, eTOCs, free email alerts (when new
articles cite this article), more»

Journals.ASM.org

Vol. 192, No. 10

The SigF Regulon in *Mycobacterium smegmatis* Reveals Roles in Adaptation to Stationary Phase, Heat, and Oxidative Stress[▽][‡]

Anja Hümpel, Susanne Gebhard,† Gregory M. Cook, and Michael Berney*

*Department of Microbiology and Immunology, Otago School of Medical Sciences, University of Otago,
P.O. Box 56, Dunedin, New Zealand*

SigF is an alternative sigma factor that is highly conserved among species of the genus *Mycobacterium*. In this study we identified the SigF regulon in *Mycobacterium smegmatis* using whole-genome microarray and promoter consensus analyses. In total, 64 genes in exponential phase and 124 genes in stationary phase are SigF dependent ($P < 0.01$, >2-fold expression change). Our experimental data reveal the SigF-dependent promoter consensus GTTT-N$_{(15–17)}$-GGGTA for *M. smegmatis*, and we propose 130 potential genes under direct control of SigF, of which more than 50% exhibited reduced expression in a Δ*sigF* strain. We previously reported an increased susceptibility of the Δ*sigF* strain to heat and oxidative stress, and our expression data indicate a molecular basis for these phenotypes. We observed SigF-dependent expression of several genes purportedly involved in oxidative stress defense, namely, a heme-containing catalase, a manganese-containing catalase, a superoxide dismutase, the starvation-induced DNA-protecting protein MsDps1, and the biosynthesis genes for the carotenoid isorenieratene. Our data suggest that SigF regulates the biosynthesis of the thermoprotectant trehalose, as well as an uptake system for osmoregulatory compounds, and this may explain the increased heat susceptibility of the Δ*sigF* strain. We identified the regulatory proteins SigH3, PhoP, WhiB1, and WhiB4 as possible genes under direct control of SigF and propose four novel anti-sigma factor antagonists that could be involved in the posttranslational regulation of SigF in *M. smegmatis*. This study emphasizes the importance of this sigma factor for stationary-phase adaptation and stress response in mycobacteria.

The success of *Mycobacterium tuberculosis* as a pathogen can be attributed to its capacity to adapt to environmental changes throughout the course of infection. These changes include nutrient deprivation, hypoxia, various exogenous stress conditions, and the intraphagosomal environment. A large cohort of genes that facilitate this adaptation has been identified, and among them are many genes for transcriptional regulators such as sigma factors that modulate gene expression in response to different physiological cues. Sigma factors interact with the RNA polymerase to allow binding to specific promoter sequences and initiation of gene transcription. Mycobacteria harbor sigma factors of only the σ^{70} family, which fall into four different categories. SigA (group 1) is the essential primary sigma factor in mycobacteria, and SigB (group 2) is its nonessential paralog. SigF (group 3) and extracytoplasmic function (ECF) sigma factors (group 4) are alternative sigma factors, which allow adaptation to a wide range of internal and external stimuli. Alternative sigma factors vary considerably in type and numbers between species, mirroring their different requirements for stress response (15).

Thirteen sigma factors have been identified in *M. tuberculosis* (23, 29). Eleven of these are classified as alternative sigma

factors, and many of them are recognized as virulence determinants. Loss of the alternative sigma factor SigF decreased the virulence of *M. tuberculosis* in mice (5) and disease-associated tissue damage in mice (13) as well as guinea pigs (20). Loss of SigF also leads to an altered cell wall composition due to a lack of virulence-related sulfolipids (13), and overexpression of *sigF* has been shown to affect the regulation of other cell wall-associated proteins involved in host-pathogen interaction (40).

SigF was originally thought to be absent in nonpathogenic, fast-growing mycobacteria such as *Mycobacterium smegmatis* (9). However, it has since become clear that SigF is well conserved among mycobacteria (30, 31) and regulates more than just virulence. While SigF is related to stress response and sporulation sigma factors in other bacteria (8), its role as a stress and stationary-phase sigma factor in *M. tuberculosis* is under debate (40).

In *M. smegmatis*, loss of *sigF* increases susceptibility to oxidative stress, acidic pH, and heat shock (12) and disables the synthesis of protective carotenoids (28). This suggests that SigF mediates a general stress response. However, there is still a paucity of basic knowledge pertaining to the SigF-regulated genes and how SigF fits into the regulatory network of sigma factors. Twenty-seven sigma factors have been proposed for *M. smegmatis* (35, 38). This is twice the number of sigma factors found in *M. tuberculosis* and possibly reflects the larger genome size and the more variable environments to which this species is required to adapt. Based on this observation, it has been suggested that the regulatory circuits involving SigF will differ between tuberculous and environmental mycobacteria given the different natures of their environments (31), but data on the regulation of SigF activity in *M. smegmatis* are lacking.

---

* Corresponding author. Mailing address: Department of Microbiology and Immunology, Otago School of Medical Sciences, University of Otago, P.O. Box 56, Dunedin, New Zealand. Phone: 64 3 479 7722. Fax: 64 3 479 8540. E-mail: michael.berney@otago.ac.nz.
† Present address: Department of Biology I, Microbiology, Ludwig-Maximilians-Universität München, Grosshaderner Strasse 2-4, 82152 Planegg-Martinsried, Germany.
‡ Supplemental material for this article may be found at http://jb .asm.org/.
▽ Published ahead of print on 16 March 2010.

In this study we report on the SigF regulon of *M. smegmatis* during exponential- and stationary-phase growth. We propose a new SigF promoter consensus for *M. smegmatis* based on our experimental data, and we identify novel target genes under the direct control of this sigma factor. We provide a rationale for the phenotypes of the Δ*sigF* strain observed in previous stress challenge experiments and propose candidate genes involved in the posttranslational regulation of SigF in *M. smegmatis*.

MATERIALS AND METHODS

Bacterial strains and growth conditions. *Mycobacterium smegmatis* strain mc²155 (33) and an isogenic *sigF* (MSMEG_1804) deletion strain (12) were routinely grown in batch culture in Luria-Bertani broth supplemented with 0.05% (wt/vol) Tween 80 (LBT) at 37°C on a rotary shaker at 200 rpm. Gentamicin was added to a final concentration of 5 μg ml^{-1} where required. Culture growth was monitored by measuring the optical density at 600 nm (OD$_{600}$). Samples were diluted in saline (8.5 g/liter NaCl) to bring the OD$_{600}$ to below 0.5 when measured in cuvettes with a 1-cm light path length in a Jenway 6300 spectrophotometer. Starter cultures were grown to exponential phase (OD$_{600}$ = 0.5 ± 0.2) and used immediately to inoculate 100 ml fresh LBT in 1-liter flasks to an initial OD$_{600}$ of 0.005.

Cell harvest. Batch cultures were harvested in exponential phase (μ = 0.26 ± 0.04 h^{-1}) and stationary phase (μ = 0.07 ± 0.01 h^{-1}) using cold glycerol-saline (36). In brief, cultures were mixed with 2 volumes of cold glycerol-saline (3:2 [vol/vol]; −20°C) and centrifuged for 20 min at 10,000 × g and −20°C. After centrifugation, the supernatant was decanted and the cells were resuspended in 1 ml glycerol-saline (1:1 [vol/vol]; −20°C), snap-frozen in a dry-ice/ethanol bath, and stored at −80°C.

RNA extraction. Total RNA was extracted with TRIzol (Invitrogen, Carlsbad, CA) following the manufacturer's recommendations. Frozen samples (−80°C) were centrifuged for 15 min at 13,000 × g and 4°C. Cells were resuspended in 1 ml TRIzol reagent and disrupted using 0.5-ml zirconium beads (0.1-mm diameter) in a Mini-BeadBeater (BioSpec Products, Bartlesville, OK) at 5,000 oscillations per min for three cycles of 30 s. The samples were chilled on ice for 30 s after each cycle. At the end of the extraction procedure, RNA pellets were air dried and redissolved in 50 μl diethyl pyrocarbonate (DEPC)-treated ultrapure water. Remaining DNA was removed with Turbo DNase (Applied Biosystems/ Ambion, Austin, TX) following the manufacturer's instructions. RNA quality was assessed by electrophoresis on a standard 1% agarose gel, and RNA quantity was determined with a NanoDrop ND-1000 spectrophotometer (Thermo Fisher Scientific, Waltham, MA).

Microarray resources. Glass slide DNA microarrays with 7,736 unique 70-mer oligonucleotides (spotted in triplicates) representing every open reading frame (ORF) of the *M. smegmatis* mc²155 genome were acquired from the Pathogen Functional Genomics Resource Center (PFGRC) established by NIAID/JCVI (http://pfgrc.jcvi.org). Standard operating procedures (SOP) for RNA labeling and array hybridization as well as layout and annotation files for the microarray were downloaded from the PFGRC website. The open-source free TM4 software suite (www.tm4.org) was used for microarray analysis.

Synthesis/labeling of cDNA. Mycobacterial RNA was aminoallyl (aa) labeled according to SOP M007 from PFGRC. In brief, cDNA was first reverse transcribed from 5 μg extracted total RNA using 3 μg random primers and SuperScript III reverse transcriptase (both from Invitrogen) with a 25 mM aa-dUTP labeling mix (2:3 aa-dUTP to dTTP). The 5-(3-aminoallyl)-dUTP was purchased from Sigma-Aldrich (St. Louis, MO). Synthesized cDNA was then coupled to either cyanine-3 or cyanine-5 (Cy-3/Cy-5) fluorescent dyes (GE Healthcare Bio-Sciences, Little Chalfont, United Kingdom) for 1 1/2 h. The concentration of cDNA and incorporation of dyes were measured with a NanoDrop ND-1000 spectrophotometer. Labeled probes were mixed and prepared as recommended for immediate hybridization to the microarray.

Microarray hybridization. The microarrays were hybridized according to SOP M008 from PFGRC except that slides were handled individually in 50-ml conical tubes instead of Coplin jars. In brief, slides were blocked for at least 2 h and washed with filtered (0.22-μm) ultrapure water, followed by a final wash with isopropanol. Wet slides were centrifuged dry for 10 min at 800 × g at room temperature. Slides were then immediately hybridized with the prepared samples and incubated for at least 18 h. After hybridization, slides were washed, centrifuged dry as described above, and immediately scanned. Wash buffers were filtered (0.22 μm) prior to use. Hybridizations comparing wild-type and Δ*sigF*

TABLE 1. Primer pairs for selected genes for real-time PCR

Locus	Gene	Primer sequence (5′ → 3′)
MSMEG_1804	*sigF*	GCTCAAGGAACTCCACTTGC (forward) GATGGACAGCGTGTTGTACG (reverse)
MSMEG_2758	*sigA*	GAAGACACCGACCTGGAACT (forward) GACTCTTCCTCGTCCCACAC (reverse)
MSMEG_2927	*opuCB*	TCTGTCGTTCCTCGCCTATC (forward) AAACCGAAGAACACCAGCAT (reverse)
MSMEG_6213	*mcat*	GGCAAGGACGAGATAATCCA (forward) TCGTCGGTGAACTGTTTGAG (reverse)
MSMEG_6232	*katA*	GCAGACCCATCTGGTCAAGT (forward) AGTTCCCATTCCGGGTAGTC (reverse)
MSMEG_6467	*dps1*	ACAACGATCTGCATCTGACG (forward) GTCACGCTCGACGGAGTAGT (reverse)
MSMEG_6515	*treS*	GGCGACTTCTACGTCTGGAG (forward) CGGGTTGTCGTAGTTGAGGT (reverse)

strains in both exponential and stationary phases were repeated in four biological replicates including dye swaps.

Image acquisition. Slides were scanned using an Axon GenePix4000B microarray scanner (Molecular Devices, Sunnyvale, CA) at a 10-μm pixel size and autoadjusted photomultiplier (PMT) gain. Fluorescences at 532 nm (Cy3) and 635 nm (Cy5) were measured simultaneously and saved in separate 16-bit grayscale TIFF images, which were then analyzed with the TM4 programs Spotfinder, MIDAS, and MEV.

Data analysis. Spots were identified with the fixed-circle segmentation method and quantified with 5% top background cutoff in Spotfinder (version 3.1.1). The spot signal intensities were normalized in MIDAS (version 2.19) using total array intensity and the LOWESS algorithm options. The gene expression ratio (*n*-fold change from Δ*sigF* strain to wild type) was calculated from the normalized signal intensities and averaged for each set of biological replicates. Ratios were tested for significance ($P < 0.05$ and $P < 0.01$) with a one-sample *t* test in MeV (version 4.3.02).

Quantitative real-time PCR. The gene expression ratios detected by microarray analysis were confirmed by quantitative real-time PCR (qRT-PCR). Selected genes and primer pairs are listed in Table 1. Gene sequences were retrieved from JCVI/CMR (http://cmr.jcvi.org/tigr-scripts/CMR/GenomePage.cgi?database=gms). Total RNA (1 μg) from stationary-phase batch cultures of *M. smegmatis* mc²155 wild-type and Δ*sigF* strains was reverse transcribed with random primers (1 μg) and SuperScript III reverse transcriptase (both from Invitrogen) according to the manufacturer's protocol. Real-time PCR was performed using a SYBR green assay (Invitrogen) and optimized primer concentrations in a 7500 fast real-time PCR system (Applied Biosystems, Foster City, CA). Relative gene expression was determined from calculated threshold cycle (C_T) values using MSMEG_2758 (*sigA*) as an internal normalization standard. *n*-fold changes were tested for significance with a Student *t* test.

Promoter search. Of 134 SigF-dependent genes (microarray analysis under standard growth conditions; $P < 0.01$, gene expression ratio $r < 0.5$), the 400-bp regions immediately 5′ to the annotated start codons were scanned visually for sequences similar to the SigF-dependent promoter upstream of MSMEG_1802 identified in our previous study (12). Such a sequence was found in 49 of these regions. For use as training sets, three separate sets, each containing all 49 promoters, were generated by adjusting the spacing between the −10 and −35 elements to 15 bp, 16 bp, or 17 bp, respectively, by deleting bases before the −10 region or by inserting an "N." These three sets were then used in separate analyses to create a custom position weight matrix (PWM) for a virtual footprint analysis of the *M. smegmatis* genome using PRODORIC (24) (http://prodoric.tu-bs.de). Search parameters were adjusted to ensure that a minimum of 80% of the training set promoters were recovered. For the 16-bp and 17-bp spacing sets, the settings were as follows: sensitivity = 0.7, core sensitivity = 0.6, and core size = 5. For the 15-bp spacing set, the settings were as follows: sensitivity = 0.8, core sensitivity = 0.6, and core size = 5. Only hits within 300 bp 5′ of an annotated start codon (JCVI/CMR) were considered. Of promoters identified by more than one of these analyses, the hits with the lower PWM score were

TABLE 2. SigF-dependent gene expression ($P < 0.01$) in *M. smegmatis* grown in LB-Tween batch cultures

Mean growth rate μ, h⁻¹, ± SD (OD₆₀₀)	SigF-dependent genes ($P < 0.01$)	No. of genes with expression in Δ*sigF* strain[a]:	
		Reduced (ratio of <0.5)	Increased (ratio of >2)
0.25 ± 0.02 (0.4 ± 0.05)	218	62 (11)	3 (3)
0.07 ± 0.01 (4.0 ± 0.2)	239	122 (71)	2 (2)

[a] The ratio is that of Δ*sigF* strain to wild-type gene expression. Genes unique to the growth phase are in parentheses.

removed, leaving a list of 130 genes. To generate a consensus sequence, all 130 identified promoters, plus the 12 promoters of the training set that were not recovered by the virtual footprint analysis, were adjusted to a spacing of 16 bp as before. This set was then used to create a sequence logo of the SigF promoter consensus using the WegLogo tool (7) (http://weblogo.berkeley.edu/logo.cgi).

Microarray data accession number. All data have been deposited at the Gene Expression Omnibus (GEJO, NCBI) under accession number GSE19145.

RESULTS AND DISCUSSION

To determine the genes of *M. smegmatis* mc²155 that are regulated by the alternative sigma factor SigF, a genome-wide gene expression study was conducted for wild-type *M. smegmatis* mc²155 and an isogenic Δ*sigF* mutant (12) using microarray analysis. Comparing these two strains, 218 and 239 genes were differentially regulated ($P < 0.01$) in exponential- and stationary-phase cells, respectively (Table 2). Using a threshold value of a >2-fold difference in gene expression, the data revealed 65 genes in exponential-phase cells and 124 genes in stationary-phase cells under SigF control (Table 3). The majority of these genes showed reduced expression in the Δ*sigF* strain, in accordance with SigF as an initiator of gene transcription. Only 3 of the 65 genes in exponential phase and 2 of the 124 genes in stationary phase had a higher expression signal in the Δ*sigF* strain. Of the 124 SigF-dependent genes in stationary-phase cells, 73 genes were exclusively identified in this growth stage, while 51 genes showed reduced expression in exponential and stationary phases. Only 14 genes were unique to the exponential-phase SigF regulon. The entire expression data can be found in Data Set S1 in the supplemental material. To validate the microarray results, we performed real-time PCR on selected genes (Fig. 1). Expression ratios showed the same trend for all genes and were significantly different from 1 ($P < 0.01$).

An improved SigF promoter consensus for *M. smegmatis*. Previous studies have identified two genes directly regulated by SigF in *M. smegmatis*: *chaB* of the *sigF* operon (12) and *crtI* of the carotenoid synthesis gene cluster (28). The promoter motif preceding both genes is identical to the SigF consensus sequence of *M. tuberculosis* (13). A further 104 SigF-regulated genes have been proposed by an *in silico* analysis of the *M. smegmatis* genome based on the SigF consensus sequence of *M. tuberculosis* (28). However, only 12 genes of this theoretical regulon, in addition to *chaB* and *crtI*, proved to be SigF dependent ($P < 0.01$) in our study, which accounted for fewer than 4% of the identified genes.

We used our microarray data to conduct a promoter motif search tailored to *M. smegmatis*. Using the SigF-dependent promoter upstream of MSMEG_1802, mapped in our previous study (12), 400 bp upstream of the annotated start codon of 134 SigF-dependent genes ($P < 0.01$ and $r < 0.5$ only) were visually checked for sequence similarities. Forty-nine possible candidate genes were found. The spacing between the −10 and −35 elements varied between 14 and 19 bp, but the majority of promoters had a spacing of 15 to 17 bp (Fig. 2A). All 49 promoters were therefore adjusted to 15, 16, or 17 bp and used as separate training sets to create custom position weight matrices for virtual footprint analysis using the PRODORIC tool (24) as described in Materials and Methods. A total of 477 sequence hits were obtained, of which 153 were located within 300 bp 5′ of an annotated start codon. Of promoters identified more than once, the hits with the lower PWM score were removed, which led to a data set of 130 separate promoters. Of these, 62 had a spacing of 15 bp, 49 had a spacing of 16 bp, and 19 had a spacing of 17 bp (Table 4). Seventy percent of promoters were located within 100 bp of the annotated start codon (Fig. 2B).

A position weight matrix of the identified promoters was created and a sequence logo for the resulting SigF consensus generated using the WebLogo tool (7) as described in Materials and Methods. This consensus for SigF-dependent promoters in *M. smegmatis* was identified as GTTT-N₍₁₅₋₁₇₎-GGGTA (Fig. 2C).

Of the 130 genes identified here, 20 had previously been proposed by Provvedi and colleagues (28) to be directly recognized by SigF, but for 6 of these the predicted promoter site differs from the site predicted by our analysis. Our consensus is supported by experimental data: 72 of the 130 genes show a significant reduction in expression ($P < 0.05$) in the Δ*sigF* strain in exponential- and/or stationary-phase cells. The remaining 58 genes carry the identified SigF promoter consensus but were not differentially expressed. They are most likely part of specific SigF-regulated stress response regulons or could represent false-positive hits.

SigF regulates genes with purported roles in oxidative stress response and pigment production. A phenotypic characteristic well established for the *M. smegmatis* Δ*sigF* strain is its pronounced sensitivity to hydrogen peroxide (12, 28). The protection against reactive oxygen species in pathogenic mycobacteria has attracted much attention due to its implication in survival within the host. The main detoxifying enzymes, catalase-peroxidase, KatG, and the alkyl hydroperoxide reductase AhpC, are conserved and well studied across the genus (16). However, none of these enzymes appear to be involved in the SigF-mediated hydrogen peroxide resistance (12). Accordingly, the *katG* and *ahpC* genes were SigF independent in the present study.

Our analysis revealed a number of alternative genes that could play a role in oxidative stress resistance in *M. smegmatis*. SigF regulates the expression of two potential H_2O_2-detoxifying enzymes: the heme-containing catalase KatA (MSMEG_6232) and a manganese-containing catalase (MSMEG_6213). Expression of both genes was 20-fold decreased in stationary-phase cells ($P < 0.01$) and 3-fold decreased in exponential-phase cells ($P < 0.05$) in the Δ*sigF* strain relative to the wild type. Neither of these catalases is found in other mycobacteria, except for a homolog of MSMEG_6213 in *M. avium*. Both enzymes supply *M. smegmatis* with an alternative route of hydrogen peroxide degradation, which is not available to other mycobacteria. Additionally, we

TABLE 3. SigF regulon ($P < 0.01$) in *M. smegmatis* grown in LB-Tween batch cultures

Gene category	Expression in $\Delta sigF$ strain	Locus	Gene product
SigF-regulated genes exclusive to stationary phase ($\mu = 0.07 \pm 0.01$ h^{-1})	Decreased[a]	MSMEG_0266	Arginine decarboxylase
		MSMEG_0267	Esterase
		MSMEG_0536	Intracellular protease, PfpI family protein
		MSMEG_0600	Dehydrogenase
		MSMEG_0637	Iron-sulfur binding oxidoreductase
		MSMEG_0670	FAD-dependent oxidoreductase
		MSMEG_0671	*S*-(Hydroxymethyl)glutathione dehydrogenase
		MSMEG_0684	Aldehyde oxidase and xanthine dehydrogenase, molybdopterin binding
		MSMEG_0963	Hypothetical protein
		MSMEG_1112	Aconitate hydratase, putative
		MSMEG_1315	Small conductance mechanosensitive ion channel (MscS) family protein
		MSMEG_1358	Conserved hypothetical protein
		MSMEG_1605	Phosphate transport system regulatory protein PhoU
		MSMEG_1766	Conserved hypothetical protein
		MSMEG_1767	Conserved hypothetical protein
		MSMEG_1768	Conserved hypothetical protein
		MSMEG_1769	UsfY protein
		MSMEG_1775	Cytochrome P450 monooxygenase
		MSMEG_1781	Hypothetical protein
		MSMEG_1783	Hypothetical protein
		MSMEG_1787	RsbW protein
		MSMEG_1792	Conserved hypothetical protein
		MSMEG_1794	Dehydrogenase
		MSMEG_1801	Hypothetical protein
		MSMEG_2160	Hypothetical protein
		MSMEG_2344	Dehydrogenase
		MSMEG_2345	Lycopene cyclase
		MSMEG_2346	Phytoene synthase
		MSMEG_2347	Phytoene dehydrogenase
		MSMEG_2376	Conserved hypothetical protein
		MSMEG_2913	Hydrolase
		MSMEG_2925	Permease membrane component
		MSMEG_2926	Glycine betaine/carnitine/choline transport ATP binding protein OpuCA
		MSMEG_3184	Malto-oligosyltrehalose trehalohydrolase
		MSMEG_3186	Glycogen-debranching enzyme GlgX
		MSMEG_3304	Succinate semialdehyde dehydrogenase
		MSMEG_3311	Acyl carrier protein
		MSMEG_3418	Conserved hypothetical protein
		MSMEG_3536	Sugar transport protein
		MSMEG_3541	Cytochrome *c* biogenesis protein transmembrane region
		MSMEG_3543	Soluble secreted antigen MPT53
		MSMEG_3560	Conserved hypothetical protein
		MSMEG_3673	4-Alpha-glucanotransferase
		MSMEG_4195	Conserved hypothetical protein
		MSMEG_4562	Conserved hypothetical protein
		MSMEG_4993	Hypothetical protein
		MSMEG_5342	Conserved hypothetical protein
		MSMEG_5343	Conserved hypothetical protein
		MSMEG_5400	Dehydrogenase
		MSMEG_5542	Transcriptional regulator, HTH_3 family protein
		MSMEG_5590	Carboxylate-amine ligase Nfa27300
		MSMEG_5606	Cytochrome *bd*-I oxidase subunit II
		MSMEG_5616	Glyoxalase/bleomycin resistance protein/dioxygenase
		MSMEG_5721	Acetyl coenzyme A acetyltransferase
		MSMEG_5826	Pyruvate decarboxylase
		MSMEG_5936	Conserved hypothetical protein
		MSMEG_6210	Conserved hypothetical protein
		MSMEG_6213	Manganese-containing catalase
		MSMEG_6232	Catalase KatA
		MSMEG_6305	Conserved hypothetical protein
		MSMEG_6354	Serine esterase, cutinase family protein
		MSMEG_6355	Hypothetical protein
		MSMEG_6501	Hypothetical protein
		MSMEG_6541	Anti-sigma factor antagonist
		MSMEG_6542	B12 binding domain protein

Continued on following page

TABLE 3—*Continued*

Gene category	Expression in Δ*sigF* strain	Locus	Gene product
		MSMEG_6612	ATPase, MoxR family protein
		MSMEG_6615	hypothetical protein
		MSMEG_6616	*S*-(Hydroxymethyl)glutathione dehydrogenase
		MSMEG_6663	C5-*O*-methyltransferase
		MSMEG_6727	Amino acid permease-associated region
		MSMEG_6728	Conserved hypothetical protein
		MSMEG_6751	Hypothetical protein
		MSMEG_6767	Mycocerosic acid synthase
	Increased[b]	MSMEG_3297	Transcriptional regulator, CadC
		MSMEG_5934	Conserved hypothetical protein
SigF-regulated genes exclusive to exponential phase (μ = 0.25 ± 0.02 h⁻¹)	Decreased	MSMEG_2343	Methylesterase
		MSMEG_3254	RDD family protein, putative
		MSMEG_3443	Hypothetical protein
		MSMEG_5078	Glucose-1-phosphate adenylyltransferase
		MSMEG_5117	Proline dehydrogenase
		MSMEG_5119	1-Pyrroline-5-carboxylate dehydrogenase
		MSMEG_5188	CAAX amino protease family protein
		MSMEG_5189	Oxidoreductase
		MSMEG_5335	Formamidase
		MSMEG_5336	Amidate substrates transporter protein
		MSMEG_5337	Putative regulatory protein, FmdB family
	Increased	MSMEG_2751	Hypothetical protein
		MSMEG_3298	Response regulator receiver domain protein
		MSMEG_3299	Putative oxidoreductase
SigF-regulated genes in both exponential and stationary phases	Decreased	MSMEG_0451	Oxidoreductase, FAD linked
		MSMEG_0672	Conserved hypothetical protein
		MSMEG_0685	Oxidoreductase, molybdopterin-binding subunit
		MSMEG_0696	Alanine-rich protein
		MSMEG_0697	Integral membrane protein
		MSMEG_1076	Conserved hypothetical protein
		MSMEG_1097	Glycosyl transferase, group 2 family protein
		MSMEG_1558	Conserved hypothetical protein
		MSMEG_1758	Hypothetical protein
		MSMEG_1770	Conserved hypothetical protein
		MSMEG_1771	Methylase, putative
		MSMEG_1772	Conserved hypothetical protein
		MSMEG_1773	Conserved hypothetical protein
		MSMEG_1774	Conserved hypothetical protein
		MSMEG_1777	UsfY protein
		MSMEG_1782	Oxidoreductase, short-chain dehydrogenase/reductase family
		MSMEG_1788	Conserved hypothetical protein
		MSMEG_1789	Conserved hypothetical protein
		MSMEG_1790	Conserved hypothetical protein
		MSMEG_1802	ChaB protein
		MSMEG_1804	RNA polymerase sigma-F factor
		MSMEG_1950	Conserved hypothetical protein
		MSMEG_1951	Conserved domain protein
		MSMEG_2112	Secreted protein
		MSMEG_2115	Conserved hypothetical protein
		MSMEG_2337	Isopentenyl-diphosphate delta-isomerase, type 2
		MSMEG_2415	Hemerythrin HHE cation binding region
		MSMEG_2830	ISMsm4, transposase
		MSMEG_2924	Permease binding protein component
		MSMEG_2927	ABC transporter, permease protein OpuCB
		MSMEG_2958	Conserved hypothetical protein
		MSMEG_3022	Transglycosylase-associated protein
		MSMEG_3185	Putative maltooligosyl trehalose synthase
		MSMEG_3255	DoxX subfamily protein, putative
		MSMEG_3419	Hypothetical protein
		MSMEG_3439	Hypothetical protein
		MSMEG_4618	Isochorismatase family protein
		MSMEG_5402	Dehydrogenase DhgA
		MSMEG_5543	Hypothetical protein
		MSMEG_5550	Protein-glutamate methylesterase
		MSMEG_5617	Immunogenic protein MPT63

Continued on following page

TABLE 3—*Continued*

Gene category	Expression in ΔsigF strain	Locus	Gene product
		MSMEG_5722	Conserved hypothetical protein
		MSMEG_5799	Nucleoside-diphosphate-sugar epimerase
		MSMEG_6211	Hypothetical protein
		MSMEG_6212	Hemerythrin HHE cation binding domain subfamily protein
		MSMEG_6467	Starvation-induced DNA-protecting protein
		MSMEG_6500	Conserved hypothetical protein
		MSMEG_6579	Conserved hypothetical protein
		MSMEG_6610	Protein of unknown function DUF58, putative
		MSMEG_6665	Integral membrane protein
		MSMEG_6819	Conserved domain protein

[a] Δ*sigF* strain/wild-type ratio of <0.5.
[b] Δ*sigF* strain/wild-type ratio of >2.

found the SigF promoter upstream of *sodA* (MSMEG_6427), encoding a superoxide dismutase, which is highly conserved in mycobacteria.

MSMEG_6467, encoding a probable starvation-induced DNA binding protein, MsDps1, exhibited reduced expression in the Δ*sigF* strain in both exponential phase ($r = 0.04$, $P < 0.01$) and stationary phase ($r = 0.03$, $P < 0.01$). Dps proteins have been linked with oxidative stress resistance in bacteria (1). MsDps1 was first identified in carbon-starved *M. smegmatis* cultures (17) and is preceded by promoter motifs recognized by the sigma factors SigF and SigH (6). A homolog of this gene can be found in other environmental mycobacteria (e.g., *M. avium*, *M. avium paratuberculosis*, or *M. kansasii*). In *B. subtilis* stress-induced production of Dps is controlled by SigB, which is the functional equivalent to mycobacterial SigF (2).

Carotenoids are able to scavenge reactive oxygen species (ROS) (42). *M. smegmatis* produces the yellow carotenoid isorenieratene under light exposure and nutrient starvation (28). The synthesis of this carotenoid was shown to be SigF dependent in *M. smegmatis* ATCC 607, and the authors suggested that this is a unique feature of that strain (28). However, our study reveals that strain mc²155 also produces this carot-

enoid (Fig. 3) and that the expression of the corresponding biosynthesis genes MSMEG_2343 to MSMEG_2347 is SigF dependent (Table 3). All genes of the cluster showed decreased expression in the Δ*sigF* strain in both growth stages (see Data Set S1 in the supplemental material). Supporting our expression data, a difference in pigmentation was observed for the mc²155 wild-type and Δ*sigF* strains when grown on LBT agar plates under illumination (Fig. 3). The wild-type colonies developed a distinct yellow color over the course of a week, whereas the Δ*sigF* strain retained its white color (Fig. 3). Complementation of the Δ*sigF* strain restored the original phenotype (data not shown).

Trehalose biosynthesis, osmoprotection, and heat stress. The microarray data suggested that seven glycosidases involved in the metabolism of trehalose and glycogen are under SigF control. Trehalose is found in a number of bacteria, where it is usually accumulated as an osmoprotectant or stored as an additional carbon source in response to stress (3, 11). In mycobacteria, trehalose is essential for growth (25, 41), and trehalose-containing glycolipids are components of their waxy, highly impenetrable cell wall (3, 11). Three different trehalose biosynthesis pathways (OtsAB, TreYZ, and TreS) have been
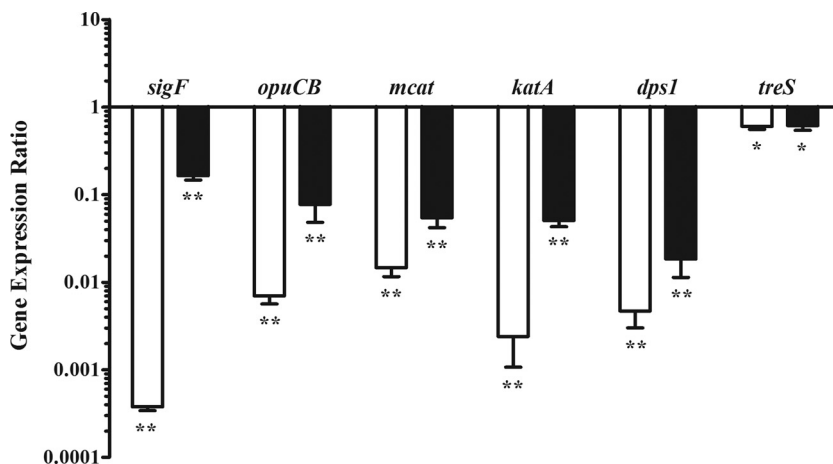
FIG. 1. Validation of microarray data with real-time PCR. Gene expression ratios (Δ*sigF* strain/wild type) of the six genes MSMEG_1804 (*sigF*), MSMEG_2927 (*opuCB*), MSMEG_6213 (*mcat*), MSMEG_6232 (*katA*), MSMEG_6467 (*dps1*), and MSMEG_6515 (*treS*) were determined by both microarray analysis (solid bars) and quantitative real-time PCR (open bars) for stationary-phase ($\mu = 0.07 \pm 0.01$) LBT batch cultures of *M. smegmatis* mc²155 wild-type and Δ*sigF* strains. Relative gene expression ratios were tested for significance (**, $P \leq 0.01$; *, $P \leq 0.05$). Results are shown as means ± standard deviations for four (solid bars) or three (open bars) biological replicates.
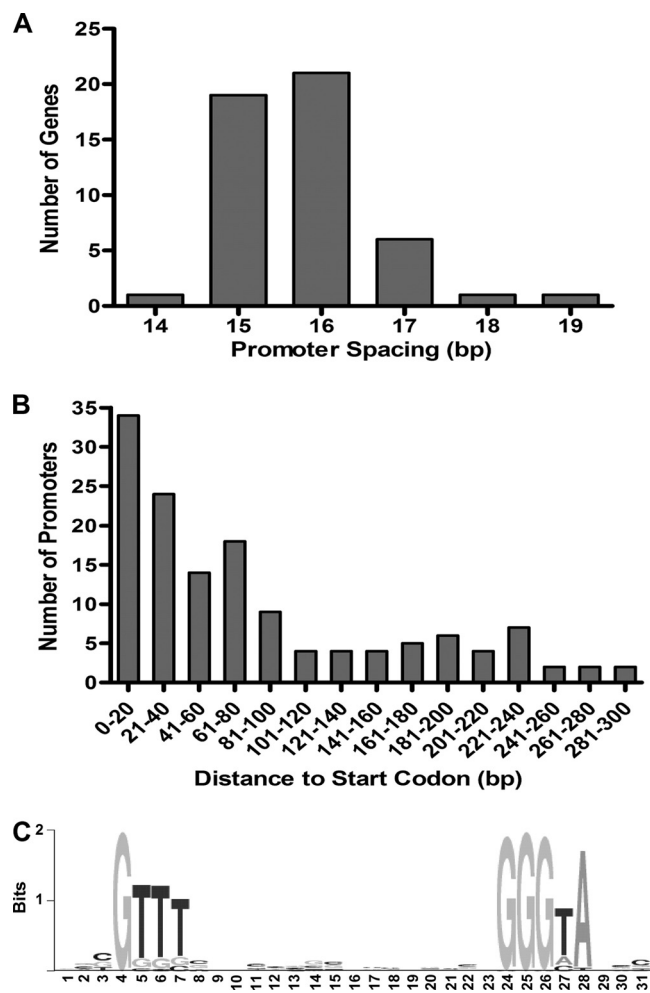
FIG. 2. Identification of the SigF promoter consensus. Visually identified promoter motifs upstream of 49 SigF-regulated genes (from microarray analysis) were used for a genome-wide virtual footprint analysis. (A) Promoter spacing variation between the −10 and −35 elements in the training set. (B) Number of promoters sorted into categories according to their distance to the start codon. (C) Derived SigF promoter consensus determined using the WebLogo tool.

characterized in *M. tuberculosis* (10) and in *M. smegmatis* (41). Two of these systems, TreS (MSMEG_6515) and TreYZ (MSMEG_3186-MSMEG_3185), showed reduced expression in the Δ*sigF* strain, and our promoter analysis further identified the TreS pathway, but not the TreYZ pathway, to be under direct control of SigF. Two genes encoding the glycogen-debranching enzyme GlgX, MSMEG_3186 (in an operon with TreYZ) and MSMEG_6507, exhibited lower expression in the Δ*sigF* strain. Glycogen is converted to trehalose by trehalose synthase (TreS). The genes of the OtsA-OtsB pathway were SigF independent in both exponential- and stationary-phase cells (see Data Set S1 in the supplemental material). Trehalose-containing glycolipids are important for cell wall integrity (26), and it has been shown that trehalose synthesis is a prerequisite for the survival of *M. smegmatis* at elevated temperatures (41). Considering this, the heat-sensitive phenotype that we observed previously for the Δ*sigF* strain (12) could be

caused by its decreased ability to synthesize trehalose as a thermoprotectant.

Furthermore, we could identify a potential system for the uptake of osmoregulatory compounds under direct control of SigF. The genes MSMEG_2927 to MSMEG_2924 are annotated as components of an ATP-binding cassette (ABC) transporter homologous to the OpuC transporter of *Bacillus subtilis* for the uptake of glycine betaine/L-proline/carnitine/choline, which is controlled by the functionally equivalent sigma factor, SigB (18, 19, 37).

Potential SigF-dependent regulators. Our promoter analysis predicted a SigF-dependent promoter sequence upstream of *sigH3* (MSMEG_0573), *whiB1* (MSMEG_1919), *whiB4* (MSMEG_6199), and *phoP* (MSMEG_5872). SigH and its paralogs have been shown to be upregulated under heat and oxidative stress in *M. smegmatis* (32). WhiB proteins are regulatory proteins unique to actinomycetes (34). In *M. tuberculosis* expression of *whiB4* has been observed at elevated temperatures (14), and WhiB1 has been similarly linked with heat and oxidative stress resistance in *Corynebacterium glutamicum* (21). Inactivation of *phoP* in *M. tuberculosis* led to an altered cell envelope composition and stress responses *in vitro*, as well as an attenuation of the pathogen *in vivo* (39). Direct control of *phoP* by SigF has been predicted previously (28), but the sequence motif we identified here is located at a different site.

Regulation of SigF. (i) Expression of the genomic region surrounding *sigF*. In *M. smegmatis*, *sigF* is part of an operon with its anti-sigma factor RsbW encoded upstream (designated UsfX in *M. tuberculosis*) and a ChaB family protein encoded upstream of *rsbW*. This arrangement of the *sigF* gene with its anti-sigma factor is conserved in mycobacteria (30). The microarray analysis showed a reduced expression of *chaB* in the Δ*sigF* strain at both time points (r < 0.24, P < 0.005), whereas *rsbW* was less compromised (r < 0.7, P < 0.02). This result is in accordance with our previous study, where we reported that *sigF* is transcribed from two different promoters: a SigF-dependent promoter preceding *chaB* and a SigF-independent promoter preceding *rsbW* (12). The lack of expression from the promoter upstream of *chaB* would have a more pronounced effect on *chaB* expression than on *rsbW* expression, as the latter is also transcribed from the SigF-independent promoter.

MSMEG_1806 (encoding a conserved hypothetical protein), directly downstream of *sigF*, was the only gene in the study with a strong increase in expression in the Δ*sigF* strain for both exponential- and stationary-phase cells (r = 12.9 and r = 21.2, respectively; P < 0.01). Most likely, the upregulation of MSMEG_1806 is due to a polar effect of the inserted gentamicin cassette (*aacC*-1) into the adjacent *sigF* gene. However, all phenotypic characteristics of the Δ*sigF* strain, which were observed in previous growth and stress challenge experiments in our laboratory (12), were reversible by complementation of the deleted *sigF* gene, rendering the increased expression of MSMEG_1806 without a noticeable impact.

(ii) Posttranslational regulation of SigF. There is little evidence of transcriptional regulation of the *rsbW*-*sigF* operon in *M. smegmatis* under standard growth conditions and for most stress conditions applied *in vitro* (12, 31). It therefore appears likely that SigF is regulated mainly at the posttranslational level. In *M. tuberculosis*, posttranslational regulation of SigF is highly complex, involving the anti-sigma factor UsfX as well as

TABLE 4. Genes of *M. smegmatis* with an identified SigF-dependent promoter consensus

Expression category	Locus	Gene product	Microarray analysis				PRODORIC promoter analysis		
			Exponential phase		Stationary phase		Promoter sequence (5' → 3')	Position[b]	PWM score[c]
			Ratio[a]	P value	Ratio	P value			
Strong SigF-dependent gene expression[e] in exponential and/or stationary phase	MSMEG_0266	Arginine decarboxylase	0.39	0.051	0.17	2.58E−04	GTCG-N17-GGGAT	160	NF
	MSMEG_0267	Esterase	0.32	0.05	0.14	4.86E−04	GTTT-N15-GGGTA	27	14.68
	MSMEG_0451	Oxidoreductase, FAD-linked	0.12	1.12E−03	0.11	9.94E−05	GTTC-N19-GGGCC	49	NF
	MSMEG_0670	FAD-dependent oxidoreductase	0.38	0.05	0.22	5.90E−03	GGTT-N16-GGGTA	9	12.99
	MSMEG_0671	S-(Hydroxymethyl)glutathione dehydrogenase	0.29	0.049	0.07	1.96E−07	GTTT-N15-GGGTA	47	14.64
	MSMEG_0672	Conserved hypothetical protein	0.19	2.29E−03	0.04	9.03E−06	GTTT-N15-GGGTA	50	14.58
	MSMEG_0697	Integral membrane protein	0.18	4.43E−03	0.04	1.48E−06	GTTT-N16-GGGAA	58	13.79
	MSMEG_1076	Conserved hypothetical protein	0.05	7.61E−06	0.03	4.16E−06	GTTT-N16-GGGTA	50	14.28
	MSMEG_1097	Glycosyl transferase, group 2 family protein	0.05	4.74E−05	0.03	1.09E−06	GTGT-N15-GGGTT	11	NF
	MSMEG_1112	Aconitate hydratase	0.36	0.06	0.19	6.42E−03	GTTT-N16-GGGTA	8	13.84
	MSMEG_1131	Tryptophan-rich sensory protein	0.29	0.04	0.82	0.63	GTGT-N16-GGGTA	9	12.95
	MSMEG_1315	Small conductance mechanosensitive ion channel family protein	0.46	0.026	0.29	1.59E−03	GTTG-N17-GGGTA	11	13.8
	MSMEG_1758	Hypothetical protein	0.26	5.15E−03	0.09	1.06E−04	GTTT-N6-GGGTA	8	14.25
	MSMEG_1766	Conserved hypothetical protein	0.57	0.1	0.15	3.66E−04	GTTT-N6-GGGAA	32	13.75
	MSMEG_1770[d]	Conserved hypothetical protein	0.04	1.28E−07	0.01	2.50E−07	GTTT-N6-GGGCA	64	13.74
	MSMEG_1771	Methylase, putative	0.08	2.49E−04	0.04	3.18E−06	GTTT-N15-GGGTA	29	14.6
	MSMEG_1773	Conserved hypothetical protein	0.19	9.80E−03	0.34	2.73E−03	GTTT-N5-GGGAA	11	14.13
	MSMEG_1774	Conserved hypothetical protein	0.1	1.06E−03	0.03	5.55E−06	GTTT-N6-GGGTA	64	14.31
	MSMEG_1775	Cytochrome P450 monooxygenase	0.34	0.07	0.09	1.07E−04	GTTT-N5-GGGTA	9	14.62
	MSMEG_1777	UsfY protein	0.15	1.44E−03	0.05	1.13E−05	GTTT-N6-GGGTA	69	14.31
	MSMEG_1782	Oxidoreductase, short chain dehydrogenase/reductase	0.19	9.73E−03	0.04	7.39E−06	GTTT-N5-GGGTA	221	14.16
	MSMEG_1787	RsbW protein	0.5	0.04	0.45	8.18E−03	GTTT-N7-GGGTA	56	14.76
	MSMEG_1792	Conserved hypothetical protein	0.44	0.11	0.16	5.01E−04	GGGT-N14-GGGCA	268	NF
	MSMEG_1794	Dehydrogenase	0.31	0.047	0.09	7.03E−05	GTGT-N17-GGGTA	15	13.28
	MSMEG_1801	Hypothetical protein	0.49	0.19	0.18	2.68E−03	GGTG-N18-GGGAA	173	NF
	MSMEG_1802	ChaB protein	0.24	5.03E−03	0.1	8.96E−05	GTTT-N6-GGGCA	63	13.6
	MSMEG_2112	Secreted protein	0.23	4.48E−03	0.31	3.52E−03	GTTT-N5-GGGTA	24	14.75
	MSMEG_2337	Isopentenyl-diphosphate delta-isomerase, type 2	0.21	3.50E−03	0.16	3.83E−04	GGTG-N15-GGGTA	67	NF
	MSMEG_2347[d]	Phytoene dehydrogenase	0.49	0.06	0.23	9.98E−04	GTTT-N16-GGGTA	97	14.4
	MSMEG_2415	Hemerythrin HHE cation binding region	0.25	3.78E−03	0.08	1.12E−05	GTTG-N5-GGGTA	61	13.42
	MSMEG_2830	ISMsm4, transposase	0.41	8.50E−03	0.54	5.29E−03	GGTT-N16-GGGTG	209	NF
	MSMEG_2913	Hydrolase	0.36	0.042	0.1	1.36E−04	GTTT-N5-GGGTA	3	14.64
	MSMEG_2927[d]	ABC transporter, permease protein OpuCB	0.17	6.18E−04	0.11	3.14E−04	GTTT-N16-GGGTA	39	14.23
	MSMEG_2958	Conserved hypothetical protein	0.17	3.78E−03	0.03	2.48E−06	GTTC-N15-GGGTA	24	13.34
	MSMEG_3022[d]	Transglycosylase-associated protein	0.05	5.77E−06	0.05	1.65E−05	GTTT-N16-GGGTA	30	14.34
	MSMEG_3082	Soul heme binding protein	0.72	7.33E−03	0.44	5.67E−03	GCTT-N16-GGGTA	67	12.94
	MSMEG_3141[d]	Conserved hypothetical protein	0.43	0.033	0.4	0.022	GTGT-N16-GGGAA	29	12.94
	MSMEG_3255	DoxX subfamily, putative	0.02	6.01E−08	0.01	8.94E−08	GTTT-N5-GGGAA	36	14.09
	MSMEG_3304	Succinate semialdehyde dehydrogenase	0.44	0.06	0.08	1.73E−07	GTGT-N15-GGGTA	25	13.24
	MSMEG_3439	Hypothetical protein	0.15	4.30E−03	0.11	3.21E−04	GTTT-N5-CGGTA	59	NF
	MSMEG_3443	Hypothetical protein	0.41	1.21E−03	0.47	0.026	GTTT-N5-GGGAT	45	NF
	MSMEG_3536	Sugar transport protein	0.56	0.07	0.29	1.33E−05	GTGG-N16-GGGTA	134	NF
	MSMEG_3543	Soluble secreted antigen MPT53	0.28	0.015	0.09	1.14E−04	GTTT-N16-GGGAA	138	13.68
	MSMEG_3673	4-Alpha-glucanotransferase	0.55	0.08	0.38	3.26E−03	GTTT-N16-GGGCA	195	13.61
	MSMEG_4195	Conserved hypothetical protein	0.58	0.017	0.42	9.23E−03	GTTT-N16-GGGTA	60	14.07
	MSMEG_5189	Oxidoreductase	0.31	6.13E−03	0.42	0.013	GGTT-N16-GGGTA	25	12.93
	MSMEG_5255	Conserved hypothetical protein	0.38	0.06	0.2	1.35E−03	GTTT-N6-GGGTA	35	NF
	MSMEG_5402	Dehydrogenase DhgA	0.21	3.45E−03	0.18	9.24E−04	GTTT-N16-GGCTA	8	14.69
	MSMEG_5543	Hypothetical protein	0.03	7.87E−07	0.02	9.61E−07	GTTT-N7-GGGTA	77	15.01
	MSMEG_5550	Protein-glutamate methylesterase	0.29	3.07E−03	0.35	9.26E−03	GTTT-N15-GGGTA	20	14.58
	MSMEG_5617	Immunogenic protein MPT63	0.02	5.65E−11	0.04	4.26E−06	GTTT-N15-GGGTA	70	14.65
	MSMEG_6211	Hypothetical protein	0.13	1.15E−03	0.06	4.79E−05	GGTT-N15-GGGTA	9	13.19
	MSMEG_6212	Hemerythrin HHE cation binding domain subfamily	0.05	2.87E−05	0.02	3.65E−07	GTTT-N15-GGGTA	51	14.64
	MSMEG_6213	Manganese-containing catalase	0.31	0.039	0.06	1.20E−05	GTTT-N15-GGGTA	40	14.57

	Gene	Annotation					Promoter		
	MSMEG_6232	Catalase KatA	0.3	0.049	0.05	1.93E−06	GTTT-N$_{16}$-GGGAA	67	13.78
	MSMEG_6305	Conserved hypothetical protein	0.31	0.028	0.12	1.11E−04	GTTT-N$_{16}$-GGGCA	8	13.55
	MSMEG_6467	Starvation-induced DNA-protecting protein	0.04	2.65E−05	0.03	3.62E−06	GTTC-N$_{16}$-GGGCA	100	NF
	MSMEG_6541	Anti-sigma factor antagonist	0.8	0.033	0.5	2.45E−03	GTTT-N$_{15}$-GGGTA	282	14.54
	MSMEG_6665	Integral membrane protein	0.18	3.16E−03	0.13	1.88E−04	GGTT-N$_{15}$-GGGAA	8	14.07
	MSMEG_6751	Hypothetical protein	0.59	0.08	0.22	3.54E−04	GCTT-N$_{16}$-GGGTA	9	13.17
	MSMEG_6768	Halogenase	0.66	0.1	0.37	0.047		9	12.88
SigF-dependent expression^f in exponential and/or stationary phase	MSMEG_0686	Oxidoreductase	0.85	0.019	0.72	0.013	GTTT-N$_{15}$-GGGTA	8	14.65
	MSMEG_1204^d	3-Oxoacyl-[acyl-carrier-protein] synthase 2	0.89	0.03	1.08	0.08	GTTC-N$_{15}$-GGGTA	128	13.27
	MSMEG_1360^d	Endonuclease/exonuclease/phosphatase	0.92	0.19	0.75	0.032	GTGT-N$_{15}$-GGGTA	14	13.25
	MSMEG_1477^d	Major facilitator superfamily	0.74	0.1	0.61	0.01	GTGT-N$_{16}$-GGGTA	122	12.93
	MSMEG_1807	Acetyl-/propionyl-coenzyme A carboxylase alpha chain	0.98	0.76	0.8	2.16E−03	GGTT-N$_{17}$-GGGTA	294	13.33
	MSMEG_1848	Formate dehydrogenase-O, major subunit	0.6	0.013	0.57	0.42	GGTT-N$_{15}$-GGGTA	8	13.22
	MSMEG_1853	Na$^+$/H$^+$ antiporter NhaA	0.69	0.026	0.66	0.023	GTTT-N$_{15}$-GGGTA	99	14.73
	MSMEG_2775	Na$^+$/H$^+$ antiporter NhaA	0.94	0.035	1.02	0.84	GTTT-N$_{16}$-GGGCA	183	13.56
	MSMEG_3046	Carbamoyl-phosphate synthase, small subunit	1.08	0.6	0.81	4.42E−03	GTTT-N$_{16}$-GGGAA	206	13.72
	MSMEG_3312	Hemerythrin HHE cation binding domain subfamily	0.74	0.08	0.56	0.025	GTTT-N$_{15}$-GGGTA	26	14.58
	MSMEG_3563^d	Drug transporter	1.14	0.83	0.61	5.64E−03	GTTT-N$_{16}$-GGGTA	114	14.21
	MSMEG_3621	NADH dehydrogenase	0.96	0.44	0.82	0.025	GTTG-N$_{15}$-GGGTA	98	13.36
	MSMEG_3689^d	Sodium:solute symporter	1.06	0.037	0.96	0.36	GTTT-N$_{16}$-GGGAA	96	13.72
	MSMEG_4831	Transcriptional regulator, TetR family protein	1.32	0.018	1.18	0.35	GTTG-N$_{16}$-GGGTA	232	12.98
	MSMEG_4918	1,4-Alpha-glucan branching enzyme	0.6	0.027	0.52	0.022	GGTT-N$_{16}$-GGGTA	172	13.2
	MSMEG_5328	Conserved hypothetical protein	0.7	0.013	0.61	0.05	GTTT-N$_{16}$-GGGAA	48	13.72
	MSMEG_5554	Antar domain protein	0.9	0.3	1.11	9.33E−03	GTTG-N$_{15}$-GGGAA	231	13.33
	MSMEG_5661	ABC transporter ATP binding protein	1.1	0.81	0.64	0.028	GTTT-N$_{16}$-GGGAA	39	13.7
	MSMEG_5710	Hypothetical protein	0.9	0.015	0.93	0.43	GTTT-N$_{16}$-GGGCA	211	12.99
	MSMEG_6515^d	Trehalose synthase	0.68	3.70E−03	0.63	0.018	GTGT-N$_{16}$-GGGTA	10	12.88
	MSMEG_6676	Probable conserved transmembrane protein	0.54	9.69E−03	0.68	0.1	GTTC-N$_{16}$-GGGTA	162	13.12
	MSMEG_6739	Hypothetical protein	0.79	0.06	0.62	0.03	GTTT-N$_{15}$-GGGTA	63	13.63
	MSMEG_6822	Beta-lactamase	0.79	9.46E−03	0.55	0.039	GTTT-N$_{16}$-GGGTA	46	14.2
No significant SigF-dependent gene expression^g observed under standard growth conditions	MSMEG_0191	BadF/BadG/BcrA/BcrD ATPase family	1.32	0.54	1.08	0.53	GTTT-N$_{17}$-GGGAA	64	14.21
	MSMEG_0362	Amidohydrolase 2	0.97	0.55	1.18	0.22	GTTC-N$_{17}$-GGGTA	69	13.43
	MSMEG_0430	ISMsm4, transposase	No data		No data		GTTT-N$_{16}$-GGGAA	155	13.75
	MSMEG_0522	pp24 protein	1.01	0.86	0.78	0.09	GTTT-N$_{15}$-GGGCA	34	14.61
	MSMEG_0681	P450 heme-thiolate protein	1.03	0.56	1	0.99	GTTT-N$_{16}$-GGGTA	45	13.02
	MSMEG_0849	Oxygenase	1.26	0.6	0.99	0.62	GTGT-N$_{17}$-GGGTA	102	13.29
	MSMEG_1055	Hexapeptide transferase family protein	No data		No data		GTGT-N$_{15}$-GGGTA	37	13.45
	MSMEG_1145	Virulence factor Mce family protein	0.97	0.22	1.15	0.43	GTTT-N$_{15}$-GGGGA	214	12.9
	MSMEG_1222	ISMsm6, transposase	1.07	0.77	1.09	0.36	GTGT-N$_{15}$-GGGTA	8	13.11
	MSMEG_1295	Transthyretin	0.76	0.06	0.8	0.08	GTGT-N$_{16}$-GGGTA	160	12.86
	MSMEG_1332	Conserved hypothetical protein	1.03	0.55	1.29	0.12	GTTT-N$_{17}$-GGGCA	161	14.24
	MSMEG_1435	Ribosomal protein S10	1.01	0.94	0.86	0.5	GTTC-N$_{15}$-GGGTA	257	13.24
	MSMEG_1440	Ribosomal protein S19	65.48	0.39	0.82	0.29	GTGT-N$_{15}$-GGGTA	354	13.17
	MSMEG_1698	Putative ammonia monooxygenase superfamily	1.93	0.33	1	0.96	GTTT-N$_{15}$-GGGTA	8	14.54
	MSMEG_1742	Oxidoreductase	0.73	0.19	0.9	0.08	GTTT-N$_{15}$-GGGTA	89	14.63
	MSMEG_1784	Type I topoisomerase	0.9	0.22	0.85	0.12	GTGT-N$_{16}$-GGGTA	183	12.91
	MSMEG_1844	Conserved hypothetical protein	0.85	0.35	0.88	0.44	GTTT-N$_{15}$-GGGTA	24	14.6
	MSMEG_1919	Transcription factor WhiB	0.85	0.08	0.86	0.37	GCTT-N$_{16}$-GGGTA	199	12.95
	MSMEG_2200^d	Formyltetrahydrofolate deformylase	1	0.91	0.97	0.71	GTTT-N$_{15}$-GGGTA	237	14.6
	MSMEG_2335	Hexapeptide transferase family protein	1.02	0.53	1.08	0.1	GTTG-N$_{17}$-GGGTA	37	13.45
	MSMEG_2425	Ammonium transporter	1.33	0.22	1.02	0.76	GTTC-N$_{15}$-GGGTA	238	13.25
	MSMEG_2466	Glutaryl coenzyme A dehydrogenase	1.17	0.17	0.96	0.79	GTTC-N$_{17}$-GGGTA	174	13.44
	MSMEG_2780	Uroporphyrinogen decarboxylase	1.05	0.6	1.02	0.71	GTTT-N$_{15}$-GGGCA	92	13.91
	MSMEG_2804	Two-component system sensor kinase	0.92	0.07	1.13	0.18	GTTG-N$_{16}$-GGGTA	39	13.13
	MSMEG_2837	Nitrate reductase NarB	0.86	0.2	0.8	0.73	GTTT-N$_{16}$-GGGTA	42	14.26
	MSMEG_2938	Acyl coenzyme A thioesterase II	1.04	0.49	1.18	0.35	GTCT-N$_{15}$-GGGTA	60	13.09
	MSMEG_3026	Conserved hypothetical protein	1.12	0.08	1	1	GTTC-N$_{15}$-GGGTA	51	13.35
	MSMEG_3205	Histidinol dehydrogenase	1.13	0.07	1.13	0.47	GCTT-N$_{15}$-GGGTA	201	13.15

TABLE 4—Continued

Expression category	Locus	Gene product	Microarray analysis				PRODORIC promoter analysis		
			Exponential phase		Stationary phase		Promoter sequence (5′ → 3′)	Position[b]	PWM score[c]
			Ratio[a]	P value	Ratio	P value			
	MSMEG_3289	gp61 protein	0.82	0.23	0.68	0.12	GTTT-N₁₅-GGGTA	29	14.68
	MSMEG_3610	Conserved hypothetical protein	1.03	0.26	1.29	0.13	GTTG-N₁₅-GGGTA	73	13.29
	MSMEG_3611	D-Xylulose 5-phosphate/D-fructose 6-phosphate phosphoketolase	1.01	0.97	0.73	0.05	GGGTT-N₁₅-GGGTA	68	13.29
	MSMEG_3672	Transporter, small multidrug resistance (SMR) family	1.12	0.41	1	0.96	GTTC-N₁₇-GGGTA	62	13.43
	MSMEG_3811	Universal stress protein family, putative	0.85	0.21	1.15	0.26	GTTG-N₁₅-GGGTA	1	13.38
	MSMEG_3822	Regulatory protein GntR, HTH	1.01	0.92	1.08	0.63	GTCT-N₁₅-GGGTA	28	13.22
	MSMEG_3918	Hypothetical protein	0.97	0.58	1.19	0.13	GTTT-N₇-GGGTA	75	14.57
	MSMEG_4070[d]	Transcriptional regulator, TetR family, putative	0.98	0.87	1.18	0.35	GTTG-N₁₆-GGGTA	69	12.94
	MSMEG_4232	UDP-N-acetylmuramoylalanyl-D-glutamate-2,6-diaminopimelate ligase	1.16	0.06	1.1	0.32	GTCT-N₁₆-GGGTA	232	12.87
	MSMEG_4270	Adenosine kinase	1.1	0.14	1.2	0.13	GTTG-N₁₆-GGGTA	246	13.08
	MSMEG_4405	Putative ECF sigma factor RpoE1	1.03	0.68	0.99	0.94	GCTT-N₁₅-GGGTA	234	13.1
	MSMEG_4427	Transmembrane efflux pump	1.11	0.47	1.15	0.35	GTTC-N₁₅-GGGAA	279	12.87
	MSMEG_4441	Cupin domain protein	1.58	0.35	1	0.99	GTCT-N₁₇-GGGTA	147	13.3
	MSMEG_4633	Peptidase S9, prolyl oligopeptidase	1.33	0.12	1.04	0.81	GTTT-N₁₆-GGGTA	95	14.16
	MSMEG_4707	Nonheme bromoperoxidase BPO-A2	0.47	0.06	0.9	0.87	GTTT-N₁₅-GGGTA	35	13.94
	MSMEG_4737	Conserved hypothetical protein	1.1	0.45	1.27	0.3	GTTG-N₁₅-GGGCA	97	13.39
	MSMEG_5011	Hypothetical protein	1.06	0.53	1.18	0.19	GGGTT-N₁₅-GGGTA	42	13.22
	MSMEG_5376	Conserved hypothetical protein	1.59	0.28	1.3	0.23	GTGT-N₁₇-GGGTA	99	13.34
	MSMEG_5434	Hypothetical protein	0.95	0.61	0.85	0.57	GGTT-N₁₅-GGGTA	119	13.16
	MSMEG_5499	Conserved hypothetical protein	1.26	0.32	1.46	0.35	GTTT-N₁₆-GGGCA	197	13.53
	MSMEG_5559	Metabolite/sugar transport protein	0.87	0.43	0.84	0.08	GTTT-N₁₆-GGGTA	39	14.12
	MSMEG_5580[d]	Ku protein	1	0.98	1.15	0.18	GTTT-N₁₆-GGGTA	9	13.67
	MSMEG_5754	gp41 protein	1.02	0.34	1	0.98	GTGT-N₁₅-GGGAA	301	12.87
	MSMEG_5773	Fatty acid desaturase	0.97	0.49	1.09	0.32	GTGT-N₁₇-GGGTA	177	13.63
	MSMEG_5872	DNA binding response regulator PhoP	1	0.96	1.2	0.05	GTTT-N₁₇-GGGTA	71	14.75
	MSMEG_5907	Acyl coenzyme A dehydrogenase	1.09	0.29	1.12	0.28	GGTT-N₁₅-GGGTA	181	13.21
	MSMEG_6091	Negative regulator of genetic competence ClpC/MecB	1.01	0.82	1.12	0.18	GTTG-N₁₅-GGGTA	136	13.42
	MSMEG_6199	Transcription factor WhiB	1.23	0.1	1.29	0.19	GCTT-N₁₅-GGGTA	23	13.14
	MSMEG_6427	Superoxide dismutase (Mn)	0.91	0.24	1.02	0.45	GGTT-N₁₇-GGGTA	120	13.3
	MSMEG_6847	Conserved hypothetical protein	0.93	0.49	1.17	0.22	GTTG-N₁₅-GGGAA	280	12.84

[a] $\Delta sigF$ strain/wild-type gene expression ratio.
[b] Base pairs between end of −10 promoter element and annotated start codon.
[c] PWM, position weight matrix. NF, not found.
[d] SigF promoter site previously proposed by Provvedi et al. (28).
[e] $P < 0.05$, >2-fold difference between wild type and $\Delta sigF$ strain.
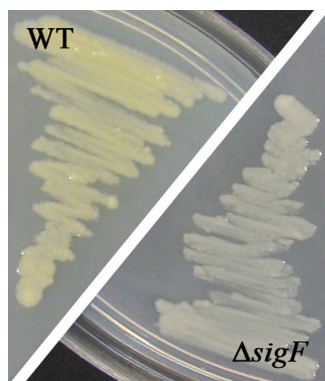[f] $P < 0.05$.
[g] $P > 0.05$.

FIG. 3. SigF-dependent pigmentation of bacterial colonies. *M. smegmatis* mc²155 wild-type (WT) and Δ*sigF* deletion strains were grown on LBT agar under standard fluorescent light at 37°C for 5 days.

five anti-sigma factor antagonists, RsfA, RsfB, Rv1364c, Rv1904, and Rv2638 (4, 27). The latter are not part of the *usfX-sigF* operon but are dispersed across the genome. To date no anti-sigma factor antagonists have been described for SigF in *M. smegmatis*.

Close inspection of our microarray data to identify potential candidates for the regulatory cascade of SigF revealed a region immediately preceding the SigF locus, where 20 of the 29 genes from MSMEG_1766 to MSMEG_1794 were affected by the *sigF* deletion ($r < 0.5$ and $P < 0.01$ in stationary phase). Furthermore, 11 of these genes were found to contain a SigF promoter. The region contains an anti-sigma factor (MSMEG_1787) with similarity to *M. smegmatis* RsbW (43% identities) and three UsfY proteins. In *M. tuberculosis*, the *usfY* gene is part of the *sigF* locus (8), but no function has been assigned to it. The close proximity of *usfY* genes to *sigF* in both *M. smegmatis* and *M. tuberculosis* indicates that the protein is involved in the control of SigF activity, although experimental evidence is missing to date.

Control of SigF activity in *M. tuberculosis* involves five anti-sigma factor antagonists. A SMART (Simple Modular Architecture Research Tool) (22) search revealed that these proteins share a STAS domain (sulfate transporter and anti-sigma factor antagonist domain). We identified four proteins with such a domain in *M. smegmatis*, either by homology to the *M. tuberculosis* anti-sigma factor antagonist RsfA (MSMEG_1786) or RsfB (MSMEG_6127) or by their annotation as STAS domain proteins (MSMEG_0586 and MSMEG_5551). A fifth STAS domain protein, MSMEG_6541, was identified from the microarray data, which showed reduced expression in the Δ*sigF* strain in stationary phase ($r < 0.5$, $P < 0.01$) and possesses a SigF-dependent promoter. None of the other four STAS domain proteins mentioned showed a change in expression in the Δ*sigF* strain. Strikingly, MSMEG_1786 (RsfA) is located in the 29-gene region upstream of *sigF*, and MSMEG_5551 is located immediately downstream of a gene under direct control of SigF (MSMEG_5550) (Table 3).

Our analysis has identified four candidate proteins as anti-SigF antagonists in *M. smegmatis*: MSMEG_1786 (based on homology to *M. tuberculosis* RsfA and the location of its gene), MSMEG_6127 (based on homology to *M. tuberculosis* RsfB), MSMEG_6541 (based on SigF-dependent expression), and MSMEG_5551 (based on the location of its gene). Together with the presence of a possible second anti-sigma factor

for SigF, MSMEG_1787, this would suggest careful fine-tuning of SigF activity, allowing the cell to exert close control over the large SigF regulon identified in this study. Future work will be required to elucidate which function each of these proteins has as part of the SigF cascade in *M. smegmatis*.

Conclusions. In this communication we report on the SigF regulon of *M. smegmatis* mc²155. We present 138 candidate genes under direct or indirect control of SigF, among them several catalase genes, the biosynthesis gene for the pigment isorenieratene, and genes for two of three trehalose-generating pathways in *M. smegmatis*. We describe a promoter consensus for 130 genes, of which more than 50% showed a reduced expression in a Δ*sigF* strain in either exponential- or stationary-phase batch cultures. We further report indications for a post-translational regulatory cascade of SigF, as predicted previously (12), and propose possible anti-SigF antagonists. In summary, this study has revealed an array of novel SigF-dependent genes which could be involved in defense against oxidative stress, heat stress, and osmotic stress in *M. smegmatis*, suggesting SigF as a key player for stationary-phase adaptation and stress response in mycobacteria.

REFERENCES

1. **Almiron, M., A. J. Link, D. Furlong, and R. Kolter.** 1992. A novel DNA-binding protein with regulatory and protective roles in starved *Escherichia coli*. Genes Dev. **6:**2646–2654.
2. **Antelmann, H., S. Engelmann, R. Schmid, A. Sorokin, A. Lapidus, and M. Hecker.** 1997. Expression of a stress- and starvation-induced dps/pexB-homologous gene is controlled by the alternative sigma factor sigmaB in *Bacillus subtilis*. J. Bacteriol. **179:**7251–7256.
3. **Arguelles, J. C.** 2000. Physiological roles of trehalose in bacteria and yeasts: a comparative analysis. Arch. Microbiol. **174:**217–224.
4. **Beaucher, J., S. Rodrigue, P. E. Jacques, I. Smith, R. Brzezinski, and L. Gaudreau.** 2002. Novel *Mycobacterium tuberculosis* anti-sigma factor antagonists control SigmaF activity by distinct mechanisms. Mol. Microbiol. **45:** 1527–1540.
5. **Chen, P., R. E. Ruiz, Q. Li, R. F. Silver, and W. R. Bishai.** 2000. Construction and characterization of a *Mycobacterium tuberculosis* mutant lacking the alternate sigma factor gene, *sigF*. Infect. Immun. **68:**5575–5580.
6. **Chowdhury, R. P., S. Gupta, and D. Chatterji.** 2007. Identification and characterization of the *dps* promoter of *Mycobacterium smegmatis*: promoter recognition by stress-specific extracytoplasmic function sigma factors SigmaH and SigmaF. J. Bacteriol. **189:**8973–8981.
7. **Crooks, G. E., G. Hon, J. M. Chandonia, and S. E. Brenner.** 2004. WebLogo: a sequence logo generator. Genome Res. **14:**1188–1190.
8. **DeMaio, J., Y. Zhang, C. Ko, and W. R. Bishai.** 1997. *Mycobacterium tuberculosis sigF* is part of a gene cluster with similarities to the *Bacillus subtilis sigF* and *sigB* operons. Tuber. Lung Dis. **78:**3–12.
9. **DeMaio, J., Y. Zhang, C. Ko, D. B. Young, and W. R. Bishai.** 1996. A stationary-phase stress-response sigma factor from *Mycobacterium tuberculosis*. Proc. Natl. Acad. Sci. U. S. A. **93:**2790–2794.
10. **De Smet, K. A., A. Weston, I. N. Brown, D. B. Young, and B. D. Robertson.** 2000. Three pathways for trehalose biosynthesis in mycobacteria. Microbiology **146:**199–208.
11. **Elbein, A. D., Y. T. Pan, I. Pastuszak, and D. Carroll.** 2003. New insights on trehalose: a multifunctional molecule. Glycobiology **13:**17R–27R.
12. **Gebhard, S., A. Hümpel, A. D. McLellan, and G. M. Cook.** 2008. The alternative sigma factor SigF of *Mycobacterium smegmatis* is required for survival of heat shock, acidic pH and oxidative stress. Microbiology **154:** 2786–2795.
13. **Geiman, D. E., D. Kaushal, C. Ko, S. Tyagi, Y. C. Manabe, B. G. Schroeder,**

R. D. Fleischmann, N. E. Morrison, P. J. Converse, P. Chen, and W. R. Bishai. 2004. Attenuation of late-stage disease in mice infected by the *Mycobacterium tuberculosis* mutant lacking the SigF alternate sigma factor and identification of SigF-dependent genes by microarray analysis. Infect. Immun. **72:**1733–1745.

14. Geiman, D. E., T. R. Raghunand, N. Agarwal, and W. R. Bishai. 2006. Differential gene expression in response to exposure to antimycobacterial agents and other stress conditions among seven *Mycobacterium tuberculosis whiB*-like genes. Antimicrob. Agents Chemother. **50:**2836–2841.

15. Gruber, T. M., and C. A. Gross. 2003. Multiple sigma subunits and the partitioning of bacterial transcription space. Annu. Rev. Microbiol. **57:**441–466.

16. Gupta, S., and D. Chatterji. 2005. Stress responses in mycobacteria. IUBMB Life **57:**149–159.

17. Gupta, S., S. B. Pandit, N. Srinivasan, and D. Chatterji. 2002. Proteomics analysis of carbon-starved *Mycobacterium smegmatis*: induction of Dps-like protein. Protein Eng. **15:**503–512.

18. Holtmann, G., and E. Bremer. 2004. Thermoprotection of *Bacillus subtilis* by exogenously provided glycine betaine and structurally related compatible solutes: involvement of Opu transporters. J. Bacteriol. **186:**1683–1693.

19. Kappes, R. M., B. Kempf, and E. Bremer. 1996. Three transport systems for the osmoprotectant glycine betaine operate in *Bacillus subtilis*: characterization of OpuD. J. Bacteriol. **178:**5071–5079.

20. Karls, R. K., J. Guarner, D. N. McMurray, K. A. Birkness, and F. D. Quinn. 2006. Examination of *Mycobacterium tuberculosis* sigma factor mutants using low-dose aerosol infection of guinea pigs suggests a role for SigC in pathogenesis. Microbiology **152:**1591–1600.

21. Kim, T. H., J. S. Park, H. J. Kim, Y. Kim, P. Kim, and H. S. Lee. 2005. The *whcE* gene of *Corynebacterium glutamicum* is important for survival following heat and oxidative stress. Biochem. Biophys. Res. Commun. **337:**757–764.

22. Letunic, I., T. Doerks, and P. Bork. 2009. SMART 6: recent updates and new developments. Nucleic Acids Res. **37:**D229–D232.

23. Manganelli, R., R. Provvedi, S. Rodrigue, J. Beaucher, L. Gaudreau, and I. Smith. 2004. Sigma factors and global gene regulation in *Mycobacterium tuberculosis*. J. Bacteriol. **186:**895–902.

24. Münch, R. H., K. A. Grote, M. Scheer, J. Klein, M. Schobert, and D. Jahn. 2005. Virtual Footprint and PRODORIC: an integrative framework for regulon prediction in prokaryotes. Bioinformatics **21:**4187–4189.

25. Murphy, H. N., G. R. Stewart, V. V. Mischenko, A. S. Apt, R. Harris, M. S. McAlister, P. C. Driscoll, D. B. Young, and B. D. Robertson. 2005. The OtsAB pathway is essential for trehalose biosynthesis in *Mycobacterium tuberculosis*. J. Biol. Chem. **280:**14524–14529.

26. Nguyen, L., S. Chinnapapagari, and C. J. Thompson. 2005. FbpA-dependent biosynthesis of trehalose dimycolate is required for the intrinsic multidrug resistance, cell wall structure, and colonial morphology of *Mycobacterium smegmatis*. J. Bacteriol. **187:**6603–6611.

27. Parida, B. K., T. Douglas, C. Nino, and S. Dhandayuthapani. 2005. Interactions of anti-sigma factor antagonists of *Mycobacterium tuberculosis* in the yeast two-hybrid system. Tuberculosis (Edinb.) **85:**347–355.

28. Provvedi, R., D. Kocincova, V. Dona, D. Euphrasie, M. Daffe, G. Etienne, R. Manganelli, and J. M. Reyrat. 2008. SigF controls carotenoid pigment production and affects transformation efficiency and hydrogen peroxide sensitivity in *Mycobacterium smegmatis*. J. Bacteriol. **190:**7859–7863.

29. Rodrigue, S., R. Provvedi, P. E. Jacques, L. Gaudreau, and R. Manganelli. 2006. The sigma factors of *Mycobacterium tuberculosis*. FEMS Microbiol. Rev. **30:**926–941.

30. Sechi, L. A., G. E. Felis, N. Ahmed, D. Paccagnini, D. Usai, S. Ortu, P. Molicotti, and S. Zanetti. 2007. Genome and transcriptome scale portrait of sigma factors in *Mycobacterium avium subsp. paratuberculosis*. Infect. Genet. Evol. **7:**424–432.

31. Singh, A. K., and B. N. Singh. 2008. Conservation of Sigma F in mycobacteria and its expression in *Mycobacterium smegmatis*. Curr. Microbiol. **56:**574–580.

32. Singh, A. K., and B. N. Singh. 2009. Differential expression of *sigH* paralogs during growth and under different stress conditions in *Mycobacterium smegmatis*. J. Bacteriol. **191:**2888–2893.

33. Snapper, S. B., R. E. Melton, S. Mustafa, T. Kieser, and W. R. Jacobs, Jr. 1990. Isolation and characterization of efficient plasmid transformation mutants of *Mycobacterium smegmatis*. Mol. Microbiol. **4:**1911–1919.

34. Soliveri, J. A., J. Gomez, W. R. Bishai, and K. F. Chater. 2000. Multiple paralogous genes related to the *Streptomyces coelicolor* developmental regulatory gene *whiB* are present in *Streptomyces* and other actinomycetes. Microbiology **146:**333–343.

35. Staron, A., H. J. Sofia, S. Dietrich, L. E. Ulrich, H. Liesegang, and T. Mascher. 2009. The third pillar of bacterial signal transduction: classification of the extracytoplasmic function (ECF) sigma factor protein family. Mol. Microbiol. **74:**557–581.

36. Villas-Boas, S. G., and P. Bruheim. 2007. Cold glycerol-saline: the promising quenching solution for accurate intracellular metabolite analysis of microbial cells. Anal. Biochem. **370:**87–97.

37. von Blohn, C., B. Kempf, R. M. Kappes, and E. Bremer. 1997. Osmostress response in *Bacillus subtilis*: characterization of a proline uptake system (OpuE) regulated by high osmolarity and the alternative transcription factor sigma B. Mol. Microbiol. **25:**175–187.

38. Waagmeester, A., J. Thompson, and J. M. Reyrat. 2005. Identifying sigma factors in *Mycobacterium smegmatis* by comparative genomic analysis. Trends Microbiol. **13:**505–509.

39. Walters, S. B., E. Dubnau, I. Kolesnikova, F. Laval, M. Daffe, and I. Smith. 2006. The *Mycobacterium tuberculosis* PhoPR two-component system regulates genes essential for virulence and complex lipid biosynthesis. Mol. Microbiol. **60:**312–330.

40. Williams, E. P., J. H. Lee, W. R. Bishai, C. Colantuoni, and P. C. Karakousis. 2007. *Mycobacterium tuberculosis* SigF regulates genes encoding cell wall-associated proteins and directly regulates the transcriptional regulatory gene *phoY1*. J. Bacteriol. **189:**4234–4242.

41. Woodruff, P. J., B. L. Carlson, B. Siridechadilok, M. R. Pratt, R. H. Senaratne, J. D. Mougous, L. W. Riley, S. J. Williams, and C. R. Bertozzi. 2004. Trehalose is required for growth of *Mycobacterium smegmatis*. J. Biol. Chem. **279:**28835–28843.

42. Ziegelhoffer, E. C., and T. J. Donohue. 2009. Bacterial responses to photooxidative stress. Nat. Rev. Microbiol. **7:**856–863.